Spectroscopic and Electrochemical Study of Copper and Zinc Complexes with a N_2S_2 Ligand Donor Set. Crystal Structure of the Copper(II) Complex derived from 1,3-Propylenediamine and 3-Formyl-1-phenyl-2(1*H*)-pyridinethione*

Michele Gullotti, Luigi Casella, Allesandro Pintar, and Edoardo Suardi
Dipartimento di Chimica Inorganica e Metallorganica, Centro CNR, Università di Milano, Via Venezian 21, 20133 Milano, Italy
Piero Zanello and Stefano Mangani
Dipartimento di Chimica, Università di Siena, Pian dei Mantellini 44, 53100 Siena, Italy

The copper(I) and zinc(II) analogues of a series of Cu^{II}–N_2S_2 complexes of bis(imine) ligands derived from the condensation of 3-formyl-1-phenyl-2(1*H*)-pyridinethione and diamines are described, together with the electrochemical properties of the couple Cu^{II}–Cu^{I} and the crystal structure of the copper(II) complex of the ligand obtained from 1,3-propylenediamine. The complex crystallizes in the centrosymmetric space group $P\bar{1}$ with a = 16.111(4), b = 11.194(4), c = 8.681(2) Å, α = 106.81(2), β = 96.47(2), γ = 95.38(2)°, Z = 2, and R = 0.073 for 3 328 reflections with $I > 3\sigma(I)$. The copper atom is equatorially co-ordinated to two imine nitrogens [Cu–N 1.980(5) and 1.989(5) Å] and two sulphur atoms [Cu–S 2.259(2) and 2.288(2) Å], and weakly bound to an oxygen atom of a perchlorate anion in an axial position [Cu–O 2.635(5) Å]. The CuN_2S_2 centre displays a slightly tetrahedrally distorted planar arrangement.

The couple Cu^{II}–Cu^{I} plays a central role in biological electron-transfer processes since copper ions are integral parts of the active sites of many proteins and enzymes involved in redox processes.[1] The crystal structure determined of *Populus nigra* plastocyanin[2] and two different azurins, from *Alcaligenes denitrificans*[3] and *Pseudomonas aeruginosa*,[4] have shown that key features of these 'blue' copper centres are sulphur (cysteine, methionine) and imidazole (histidine) co-ordination in low-symmetry environments. These structural features markedly facilitate the change of redox state of the copper ion but the details of the thermodynamic and kinetic aspects of the electron transfers are far from being understood.[5] The characterization of the 'blue' protein sites has stimulated much research interest in synthetic, low-molecular-weight complexes with CuN_2S_2 cores,[5–10] because in these systems it is easier to rationalize the various factors relating structural preferences and redox reactivity.

We have recently reported several Cu^{II}–N_2S_2 systems, where the sulphur donor atoms are provided by pyridinethione residues, with pyridinium thiolate character, and the nitrogen donors by imine groups, which can be represented schematically by structures (**1**) and (**2**).[11] Together with other systems with Cu^{II}–N_2SS^* cores,[12] also derived from pyridinethione ligands, these complexes provide a framework to investigate structural–spectral and electrochemical relationships of relevance in the biomimetic chemistry of blue copper sites. The current use of the pyridinethione residue as a mimic for the aliphatic thiolate ligand present in proteins is dictated by the necessity to overcome the redox instability of simple, synthetic copper(II)-aliphatic thiolate systems,[13] but our future efforts will be directed toward the synthesis of sterically protected aliphatic carbonyl thiols in an attempt to obtain more stable copper(II) complexes. In the present paper we complete the characterization of systems of types (**1**) and (**2**) by reporting the crystal structure determination of a member of group (**1**) with

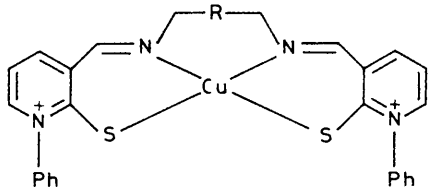

(**1**)

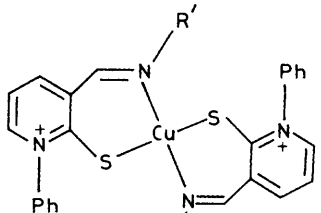

(**2**)

a trimethylene bridge R between the imine nitrogens, the synthesis of complexes of Cu^{I} and Zn^{II}, and the electrochemical behaviour of the Cu^{II}–Cu^{I} couples. The symbols employed for the various ligands are summarized in Scheme 1.

Results and Discussion

Description of the Crystal Structure of $[CuL^2(ClO_4)][ClO_4]$.—The structure consists of $[CuL^2(ClO_4)]^+$ cations and disordered ClO_4^- anions. A plot of the cation together with the labelling scheme is shown in Figure 1. The copper(II) ion is co-ordinated by two nitrogen and two sulphur atoms of the ligand; a weakly bound oxygen of a perchlorate anion completes the co-ordination polyhedron. The CuN_2S_2 core displays a slightly tetrahedrally distorted planar geometry, the dihedral angle between the planes defined by N(8)–Cu–N(12) and S(1)–Cu–S(2) being 19.6(2)°. The Cu^{II} is only 0.072(1) Å out

* *Supplementary data available:* see Instructions for Authors, *J. Chem. Soc., Dalton Trans.*, 1989, Issue 1, pp. xvii—xx.

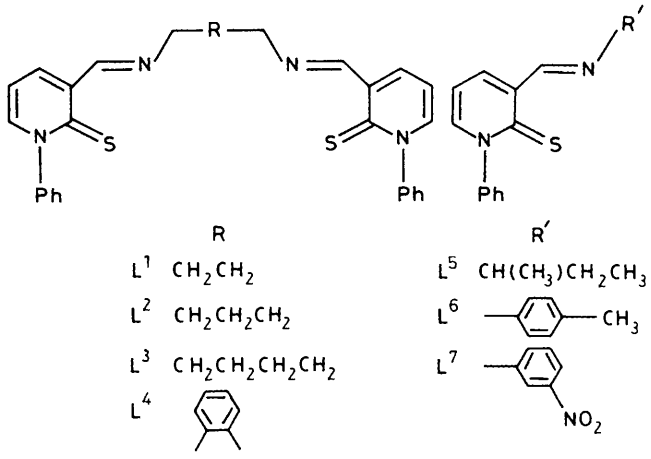

Scheme 1.

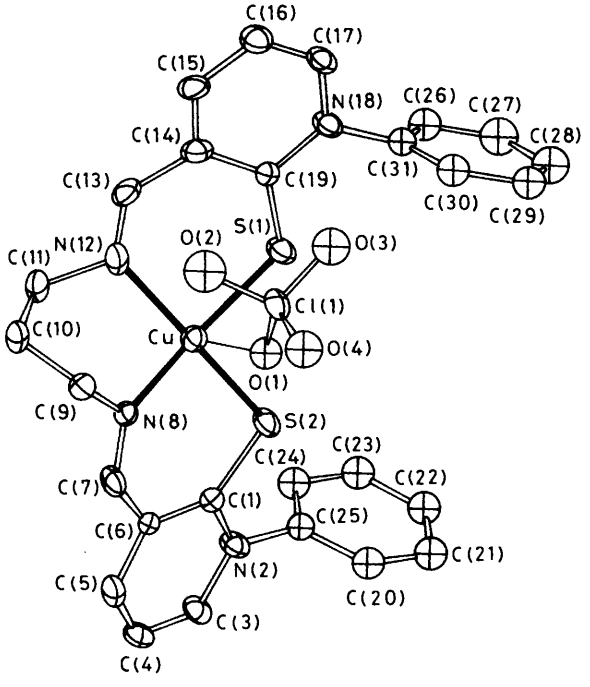

Figure 1. ORTEP diagram of $[CuL^2(ClO_4)]^+$ with atomic labelling. Thermal ellipsoids are drawn at 30% probability. Hydrogen atoms are omitted for clarity

of the mean plane of the ligand atoms toward the perchlorate oxygen. The very weak Cu^{II}–$OClO_3$ interaction does not produce the characteristic splitting of perchlorate vibrations in the i.r. spectrum of the compound;[11] it is likely that solvent molecules replace the perchlorate group in the weak apical co-ordination site in solution. The main features of the CuN_2S_2 co-ordination environment are in full agreement with those deduced from the spectroscopic properties of the complex in solution.[11]

Bond distances and angles are reported in Table 1. The Cu–S distances of 2.26 and 2.29 Å compare with those of copper–heterocyclic thiolates (2.25 Å)[9d] and –dithiocarboxylates (2.22—2.26 Å),[10] and are in the middle of the range observed for copper–aliphatic and –aromatic thiolates (2.13—2.42 Å),[8e,14] including plastocyanin.[15] The Cu–S bond distance estimated by extended *X*-ray absorption fine structure (EXAFS) for cytochrome *c* oxidase (2.27 Å) is also in this range.[16] In making these comparisons it should be taken into account that the pyridinethione imine is a neutral ligand, while the thiolate ligands carry negative charge; the Cu–S bonds in $[CuL^2(ClO_4)]^+$ are thus rather strong. The Cu–S–C angles, which are a measure of the hybridization at the sulphur atoms, are near 107° and are similar to those of a few copper(II) thiolates[9d,14b] and plastocyanin,[15] while for other synthetic copper(II) thiolates such angles deviate substantially from this value.[14a,c,d] The Cu–N bond lengths are in the normal range found for copper(II)–imine complexes.[17]

In the ligand molecule both pyridine rings deviate somewhat from ideal aromatic geometry: distances from 1.34 to 1.43 Å and bond angles from 115 to 123°. This observation, together with the two short C–S distances of 1.69 and 1.71 Å, may suggest substantial pyridinethione character in the ligand. However, the largest and shortest C–C distances within the pyridine rings belong to the bonds which are closest and most distant from the metal, respectively. This is quite usual in the aromatic ring structure of copper(II)–salicylaldimine complexes.[17] In addition, the five ligand atoms belonging to the six-membered chelate rings containing the sulphur atoms lie in a common plane and are almost coplanar with the adjacent pyridine rings, while the Cu^{II} is displaced from those planes by only 0.6 and 0.8 Å, respectively. This indicates that a certain degree of π delocalization occurs between the adjacent chelate and pyridine rings of the ligand, as is confirmed by the short C(6)–C(7) and C(13)–C(14) single-bond distances of 1.45 and 1.46 Å respectively, and the long C(1)–C(6) and C(14)–C(19) aromatic bond distances of 1.43 and 1.42 Å respectively. Therefore, we believe that the non-negligible contribution to the shortening of the C–S bonds comes from π delocalization within the chelate rings, and still prefer the formalism of depicting the ligands of pyridinethione complexes in their pyridinium thiolate forms. The change in formalism is suggested by some major changes occurring in the spectral properties of the ligands on metal binding, as shown previously for a related series of complexes[12a] and confirmed here by comparison of the spectra of the ligand L^1 and of several zinc(II) complexes (see later).

Characterization of the Copper(I) *and Zinc*(II) *Complexes.*—In a previous paper[11] we investigated the effect of the substituents R and R′ in the pyridinethione imine ligands on the structure of the resulting copper(II) complexes (**1**) and (**2**) respectively. For complexes of type (**1**) it was found that on extending the length of the carbon chain R a progressive distortion of the copper(II) chromophore from square planar to flattened tetrahedral results, while the structure of complexes of type (**2**) is much less dependent on the nature of the substituents R′. In both cases the structural features of the complexes could be inferred from the rich spectroscopic characteristics of Cu^{II}. Since copper(I) complexes are diamagnetic and generally exhibit poor optical properties, we thought it of interest to see if it was possible to find any spectroscopic probe for the structure of the copper(I) counterparts of (**1**) and (**2**). Some representative copper(I) complexes were thus synthesized (Table 2) and compared with the corresponding zinc(II) complexes; these are the appropriate reference for the electronic structure and spectra of the ligands in the copper(II) systems.

The complexes of Cu^I and Zn^{II} were obtained by adding the perchlorate salts of the metals to preformed solutions of the Schiff bases. The copper(I) complexes appear reasonably air-stable both in the solid state and in solution. The i.r. spectra of the complexes display broad, featureless bands near 1 100 cm^{-1}, which are indicative of non-co-ordinated perchlorate, and characteristic imine ν(C=N) bands in the range 1 620—1 650 cm^{-1}. Particularly rich are the i.r. regions in which the ring stretching modes (1 480—1 610 cm^{-1}) and out-of-plane C–H bending modes (below 900 cm^{-1}) occur due to the presence of several aromatic nuclei in the ligands.

The changes undergone by the pyridinethione imine ligands

Table 1. Selected bond lengths (Å) and angles (°) for $[CuL^2(ClO_4)][ClO_4]$

Cu–S(1)	2.288(2)	C(17)–N(18)	1.364(8)	C(9)–C(10)	1.53(1)	N(2)–C(3)	1.383(9)
Cu–N(12)	1.989(5)	C(19)–C(14)	1.420(9)	N(12)–C(13)	1.253(9)	C(4)–C(5)	1.36(1)
C(1)–N(2)	1.359(8)	Cu–S(2)	2.259(2)	C(15)–C(16)	1.38(1)	C(7)–N(8)	1.281(8)
N(2)–C(25)	1.431(7)	Cu–O(1)	2.635(5)	N(18)–C(19)	1.383(8)	C(10)–C(11)	1.51(1)
C(5)–C(6)	1.38(1)	C(1)–C(6)	1.430(9)	C(19)–S(1)	1.691(6)	C(13)–C(14)	1.46(1)
N(8)–C(9)	1.475(8)	C(3)–C(4)	1.34(1)	Cu–N(8)	1.980(5)	C(16)–C(17)	1.34(1)
C(11)–N(12)	1.469(9)	C(6)–C(7)	1.446(9)	C(1)–S(2)	1.711(6)	N(18)–C(31)	1.437(7)
C(14)–C(15)	1.38(1)						
S(1)–Cu–S(2)	86.0(1)	C(19)–C(14)–C(13)	123.5(6)	C(7)–N(8)–Cu	129.9(5)	C(6)–C(1)–S(2)	126.4(5)
N(12)–Cu–S(1)	92.7(2)	C(17)–C(16)–C(15)	117.4(7)	C(10)–C(9)–N(8)	110.9(7)	C(25)–N(2)–C(3)	116.0(5)
O(1)–Cu–S(1)	89.0(1)	C(31)–N(18)–C(17)	115.3(5)	C(11)–N(12)–Cu	113.5(5)	C(6)–C(5)–C(4)	123.0(7)
O(1)–Cu–N(12)	102.9(2)	N(18)–C(19)–S(1)	117.7(5)	C(14)–C(13)–N(12)	128.9(7)	C(7)–C(6)–C(5)	116.2(6)
N(2)–C(1)–S(2)	116.9(5)	N(8)–Cu–S(2)	94.8(2)	C(19)–C(14)–C(15)	120.4(7)	C(9)–N(8)–Cu	113.9(4)
C(3)–N(2)–C(1)	122.7(5)	N(12)–Cu–S(2)	162.8(2)	N(18)–C(17)–C(16)	122.2(7)	C(11)–C(10)–C(9)	113.1(6)
C(4)–C(3)–N(2)	121.1(7)	O(1)–Cu–S(2)	94.3(1)	C(31)–N(18)–C(19)	121.5(5)	C(13)–N(12)–Cu	128.5(5)
C(5)–C(6)–C(1)	118.6(6)	C(19)–S(1)–Cu	106.1(2)	N(18)–C(19)–C(14)	114.9(6)	C(15)–C(14)–C(13)	116.1(7)
N(8)–C(7)–C(6)	128.1(6)	N(2)–C(1)–C(6)	116.7(5)	N(8)–Cu–S(1)	171.0(2)	C(16)–C(15)–C(14)	122.2(8)
C(9)–N(8)–C(7)	116.2(6)	C(25)–N(2)–C(1)	121.3(5)	N(12)–Cu–N(8)	89.2(2)	C(19)–N(18)–C(17)	123.0(6)
N(12)–C(11)–C(10)	111.4(7)	C(5)–C(4)–C(3)	118.0(7)	O(1)–Cu–N(8)	82.0(2)	C(14)–C(19)–S(1)	127.4(5)
C(13)–N(12)–C(11)	117.8(6)	C(7)–C(6)–C(1)	125.2(6)	C(1)–S(2)–Cu	107.5(2)		

Table 2. Elemental analyses[a] and selected i.r. bands[b] for the copper(I) and zinc(II) complexes

	Analysis/%			I.r. (cm^{-1})			
Compound	C	H	N	ν(C=N)	ν(ring)	ν(ClO_4)	δ(CH)
L^1	68.7	4.50	11.95	1 638	1 606, 1 592,		756, 740,
	(68.4)	(4.80)	(12.25)		1 535, 1 491		690
$[CuL^1][ClO_4]$	50.3	3.70	8.95	1 631	1 598, 1 590,	1 088,	764, 717,
	(50.55)	(3.60)	(9.05)		1 541, 1 488	622	693
$[CuL^2][ClO_4]$	51.0	3.95	8.70	1 632	1 598, 1 590,	1 087,	762, 719,
	(51.35)	(3.85)	(8.85)		1 543, 1 489	623	694
$[CuL^3][ClO_4]$	51.85	4.00	8.55	1 635,	1 598, 1 590,	1 086,	762, 719,
	(52.1)	(4.05)	(8.70)	1 628	1 540, 1 489	623	694
$[CuL^6{}_2][ClO_4]$	58.9	4.05	7.15	1 618	1 587, 1 558, 1 540,	1 087,	820, 762,
	(59.15)	(4.20)	(7.25)		1 503, 1 489	623	719, 694
$[ZnL^1][ClO_4]_2$	43.1	3.30	7.70	1 649	1 601, 1 590,	1 095,	762, 723,
	(43.45)	(3.10)	(7.80)		1 557, 1 488	621	694
$[ZnL^2][ClO_4]_2$	44.65	3.60	7.65	1 648,	1 598, 1 590,	1 090,	768, 762,
	(44.25)	(3.30)	(7.65)	1 642	1 552, 1 489	623	723, 693
$[ZnL^3][ClO_4]_2$	44.9	3.70	7.50	1 646	1 600, 1 591,	1 097,	764, 723,
	(45.0)	(3.50)	(7.50)		1 560, 1 490	624	696
$[ZnL^6{}_2][ClO_4]_2$	52.0	3.80	6.35	1 621	1 600, 1 588, 1 558,	1 093,	821, 762,
	(52.25)	(3.70)	(6.40)		1 505, 1 489	623	722, 695

[a] Calculated values in parentheses. [b] All bands are of medium or strong intensity.

Table 3. Electronic spectra of copper(I) and zinc(II) complexes in acetonitrile solution

Compound	$\lambda_{max.}$/nm (ε/dm^3 mol^{-1})
L^1	317 (24 600), 409 (7 500)
$[CuL^1][ClO_4]$	290 (sh) (12 500), 309 (12 950), 380 (8 100), 550 (2 650)
$[CuL^2][ClO_4]$	290 (sh) (13 000), 308 (13 800), 400 (6 400), 515 (sh) (3 150)
$[CuL^3][ClO_4]$	295 (15 500), 305 (sh) (15 400), 403 (5 840), 480 (5 100)
$[CuL^6{}_2][ClO_4]$	326 (25 000), 419 (10 200)
$[ZnL^1][ClO_4]_2$	310 (sh) (13 200), 332 (17 600), 365 (sh) (13 000)
$[ZnL^2][ClO_4]_2$	321 (16 250), 365 (sh) (10 800)
$[ZnL^3][ClO_4]_2$	323 (15 800), 365 (sh) (9 600)
$[ZnL^6{}_2][ClO_4]_2$	324 (23 100), 379 (15 800)

on binding to a metal become evident on comparison of the spectral properties of the free ligand L^1 and of the complexes of Cu^I and Zn^{II} with L^1—L^3 (Tables 2—4). The increase in pyridinium thiolate character is indicated by the blue shift of the lowest-energy near-u.v. electronic absorption of the ligand (≈410 nm), due to an aromatic π ⟶ π* transition, on binding to Cu^I (380—400 nm) and especially Zn^{II} (≈365 nm), and by the downfield shift of the ring proton n.m.r. signals resulting from the aromatization and increased positive charge on the pyridine nucleus that accompanies metal binding. Both effects are larger in the zinc(II) complexes because of their higher overall positive charge. In these systems more positive charge is obviously also localized on the metal, as evidenced by the larger downfield shifts of the n.m.r. signals of the ligand groups adjacent to the donor atoms (CH=N and CH_2–N). Considering the position of the azomethine proton signal, it should be noted that this signal is found at unusually low field for the free ligand, due to the presence of different electronic effects in the thione form, and, therefore, it cannot be compared directly with those of its metal complexes.[12a]

Analysis of the spectroscopic data for the zinc(II) complexes in Tables 2—4 shows no significant variation throughout the series, whereas for the copper(I) compounds a regular variation in the position of the electronic band at lowest energy may be indicative of structural changes in the series $[CuL^1]^+$ to

Table 4. Proton n.m.r. spectra of copper(I) and zinc(II) complexes in CD_3CN[a]

Compound	CH=N	Pyridine and phenyl H	CH_2–N	C–CH_2–C	CH_3	*J*
L^1	8.98 (s)	6.7—8.1 (m)	3.90 (s)			
$[CuL^1][ClO_4]$	8.45 (br)	6.9—8.1 (m)	3.95 (br)			
$[CuL^2][ClO_4]$	8.35 (≈s)	6.9—8.1 (m)	3.60 (≈t)	*b*		5.9
$[CuL^3][ClO_4]$	8.38 (s)	6.9—8.1 (m)	3.75 (≈t)	2.0—2.4 (m)[b]		≈5
$[CuL^6{}_2][ClO_4]$	8.47 (≈s)	7.0—8.2 (m)			2.35	
$[ZnL^1][ClO_4]_2$	8.86 (≈s)	7.2—8.5 (m)	4.13 (≈s)			
$[ZnL^2][ClO_4]_2$	8.70 (≈s)	7.2—8.5 (m)	4.08 (≈t)	*b*		5.8
$[ZnL^3][ClO_4]_2$	8.78 (≈s)	7.2—8.5 (m)	4.05 (m)	2.0—2.4 (m)[b]		
$[ZnL^6{}_2][ClO_4]_2$	8.77 (s)	6.9—8.5 (m)			2.33	

[a] All chemical shift data referenced to $SiMe_4$; coupling constants are given in Hz. [b] Obscured by solvent absorption.

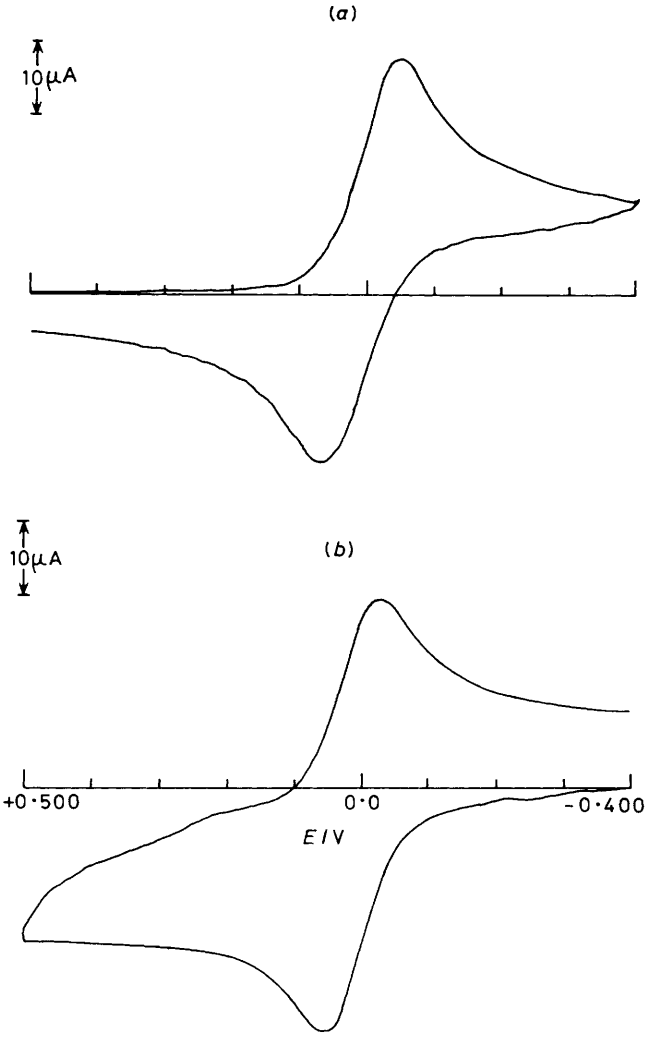

Figure 2. Cyclic voltammograms recorded at a platinum electrode on deaerated acetonitrile solutions containing NEt_4ClO_4 (0.1 mol dm^{-3}) and (*a*) $[CuL^2]^{2+}$ (1.40×10^{-3} mol dm^{-3}), (*b*) $[CuL^2]^+$ (1.30×10^{-3} mol dm^{-3}). Scan rate 0.5 V s^{-1}

$[CuL^3]^+$. This band has a moderate intensity and is missing in the spectra of the zinc(II) complexes; we therefore assign it to metal-to-ligand charge-transfer (m.l.c.t.) transitions from the filled *d* levels of Cu^I to the lowest π^* orbital of the conjugated imine ligand. These transitions occur at much higher energy for the zinc(II) complexes and fall outside the near-u.v. region investigated.

Since the electronic chromophore of the ligand is unchanged in the series L^1—L^3, the variation in the position of the m.l.c.t. band must reflect the change in energy of the copper(I) *d* orbitals determined by differences in the structures of the complexes. While complexes of Cu^I and Zn^{II} prefer to assume a tetrahedral geometry, the short ethylenediamine bridge of L^1 may not allow more than a slight tetrahedral distortion of the $[CuL^1]^+$ complex and it is likely that an almost regular tetrahedral arrangement is accessible to the Cu^I only with the four-carbon bridge of L^3. Since the energy of the highest *d* orbitals decreases with the distortion of a square-planar field toward a tetrahedron, the position of the m.l.c.t. transition is expected to undergo a corresponding shift to high energy, as observed here in the series $[CuL^1]^+$ to $[CuL^3]^+$. In agreement with this interpretation, the m.l.c.t. band occurs at still higher energy for $[CuL^6{}_2]^+$, which is certainly allowed to assume a perfectly regular tetrahedral geometry, even though the presence of a conjugated phenyl residue in L^6 makes a direct comparison with the chromophore of L^1—L^3 less straightforward.

Electrochemistry of the Copper(II)–Copper(I) Couples.—The electrochemical behaviour of $[CuL^1]^{2+}$ was examined some time ago in dimethylformamide solution.[9a] The most significant feature of the redox behaviour of the derivatives $[CuL^1]^{2+}$ to $[CuL^4]^{2+}$ is the couple Cu^{II}–Cu^I. Figure 2(*a*) shows as a typical example of the cyclic voltammetric response exhibited by $[CuL^2]^{2+}$ at a platinum electrode in acetonitrile solution. The full chemical reversibility of the one-electron reduction is testified by the complementary response exhibited by $[CuL^2]^+$, Figure 2(*b*). Confirming the chemical evidence, controlled-potential coulometric tests performed at −0.3 V indicate the reduction process to involve one electron per molecule of $[CuL^2]^{2+}$; in addition, the cyclic voltammogram recorded on the exhaustively reduced reddish solution is similar to that shown in Figure 2(*b*).

Analysis of the cyclic voltammetric responses with scan rates varying from 0.02 to 20.480 V s^{-1} gives evidence for a quasi-reversible electron transfer, uncomplicated by subsequent chemical reactions.[18] The i_{p_a}/i_{p_c} ratio is constant at unity, the current function $i_{p_c}v^{-\frac{1}{2}}$ is substantially constant, and the difference $\Delta E_p = E_{p_a} - E_{p_c}$ gradually increases from 75 mV at 0.02 V s^{-1} to 340 mV at 20.480 V s^{-1}. As shown in Figure 3, another ill defined, subsequent cathodic step at $E_p = -1.1$ V follows the reduction Cu^{II}–Cu^I. The presence of the stripping peak at −0.25 V in the reverse scan clearly allows assignment to the reduction Cu^I–Cu^0, followed by a rapid demetallation process.

A final interesting aspect of the redox activity of the complexes $[CuL^1]^{2+}$ to $[CuL^4]^{2+}$ is their anodic oxidation. Except for $[CuL^1]^{2+}$, all complexes undergo in acetonitrile solution a

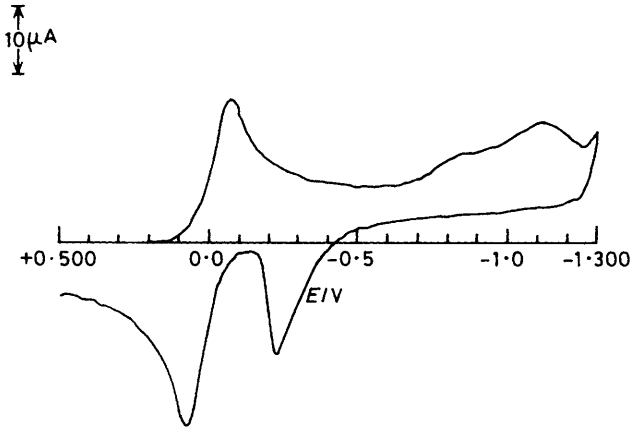

Figure 3. Cyclic voltammogram recorded at a platinum electrode on a deaerated acetonitrile solution containing $[CuL^2]^{2+}$ (1.40×10^{-3} mol dm^{-3}) and NEt_4ClO_4 (0.1 mol dm^{-3}). Scan rate 0.2 V s^{-1}

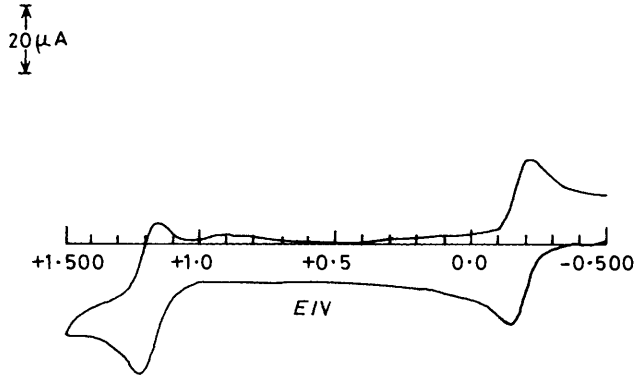

Figure 4. Cyclic voltammogram recorded at a platinum electrode on an acetonitrile solution containing $[CuL^1]^+$ (1.30×10^{-3} mol dm^{-3}) and NEt_4ClO_4 (0.1 mol dm^{-3}). Scan rate 0.2 V s^{-1}

first irreversible one-electron oxidation, followed by other ill defined anodic processes. Comparison with the redox behaviour of their zinc(II) analogues, which are anodically redox silent below +1.4 V (while displaying an irreversible reduction at the zinc centre around −1.1 V), allows us to attribute this first step to a metal-centred process, *i.e.* it corresponds to the oxidation Cu^{II}–Cu^{III} (for $[CuL^2]^{2+/3+}$, $E_p = +1.15$ V; for $[CuL^3]^{2+/3+}$, $E_p = +1.20$ V; for $[CuL^4]^{2+/3+}$, $E_p = +1.05$ V). This oxidation presents features of chemical reversibility only in the case of $[CuL^1]^{2+}$, as shown in Figure 4. This is not unexpected; taking into account that copper(III) species are planar, only the $[CuL^1]^{2+}$ ion is stereochemically suitable for such a redox change.

Analysis of the cyclic voltammograms for this Cu^{II}–Cu^{III} response ($E^{\circ\prime} = +1.18$ V) at varying scan rates reveals that it is complicated by decomposition of the copper(III) species. Assuming a first-order decomposition process, a half-life of about 1 s can be computed for $[CuL^1]^{3+}$.[18] In dimethylformamide (dmf) solution the complexes $[CuL^1]^{2+}$ to $[CuL^4]^{2+}$ behave essentially in the same manner. The only difference is that no electrode deposition of copper metal occurs in correspondence to the step Cu^I–Cu^0, even if such a process is irreversible in character. In addition, concerning the complex $[CuL^1]^{2+}$, its copper(III) species is notably less long-lived in dmf than in MeCN.

Table 5 summarizes the electrode potentials for the most significant redox change, Cu^{II}–Cu^I, of the complexes $[CuL^1]^{2+}$ to $[CuL^4]^{2+}$ both in acetonitrile and dimethylformamide solutions. Also reported is the difference between the forward and backward peaks, which, if compared with the value of 59 mV for a purely reversible one-electron transfer, can provide a rough evaluation of the degree of reversibility of the relevant one-electron addition.

Table 5. Significant electrochemical parameters for the redox change Cu^{II}–Cu^I of the complexes $[CuL^1]^{2+}$ to $[CuL^4]^{2+}$ in different non-aqueous solvents[a]

	MeCN		dmf	
Complex	$E^{\circ\prime}$/V	ΔE_p[b]/mV	$E^{\circ\prime}$/V	ΔE_p[b]/mV
$[CuL^1]^{2+}$	−0.17	80	−0.18	90
			−0.22[9a]	60[9a]
$[CuL^2]^{2+}$	+0.01	85	+0.01	85
$[CuL^3]^{2+}$	+0.20	81	+0.19	83
$[CuL^4]^{2+}$	+0.24	110	+0.21	210

[a] Redox potentials *vs.* s.c.e. Under the present experimental conditions the ferrocenium–ferrocene couple was located at +0.38 and +0.45 V in acetonitrile and dimethylformamide solutions, respectively. [b] Peak separation measured at 0.2 V s^{-1}.

The structural reorganizations accompanying a redox change should affect essentially the kinetics of the heterogeneous electron-transfer process. According to the Marcus theory, inner-sphere rearrangements, enhancing the activation barrier of the electron transfer, slow down the rate of the process, so causing a departure from electrochemical reversibility.[19] However, Gray has elegantly pointed out that the lower is the reorganization following a redox change in copper complexes the more positive is its thermodynamic redox potential.[20]

In the present series of complexes the largest rearrangement is likely experienced by the planar $[CuL^1]^{2+}$.[11] An increase in length of the bridging carbon chain, R, inducing increased tetrahedral distortion in the relevant copper(II) species, makes it easier to access Cu^I. Regarding the derivative $[CuL^4]^{2+}$, even if steric repulsion between the hydrogen atoms of the bridging phenyl and the hydrogen atoms α to the imine groups may induce some tetrahedral distortion, as evidenced by spectroscopic data,[11] we think that the high redox potential arises mainly from electronic effects due to the electron-withdrawing ability of the phenyl group.

Gray and co-workers[21] have shown that in the one-electron reduction of blue copper proteins in aqueous solutions (pH 6.5—7.0) the entropy change associated with the change Cu^{II}–Cu^I is negative (−24 for stellacyanin, −32 for plastocyanin, −43 cal K^{-1} mol^{-1} for azurin). The negativity of this value is attributed to the fact that the copper site is buried in an hydrophobic environment, which inhibits the release of water molecules following the partial charge neutralization and prevents a decrease in solvent ordering. In simple biomimetic model complexes such environmental effects are not expected. In order to test this hypothesis we have measured the entropy change for the Cu^{II}–Cu^I redox couple of $[CuL^2]^{2+/+}$ and $[CuL^3]^{2+/+}$, which should best mimic the corresponding structural change in the active site of the blue copper proteins.[22] The entropy of the charge transfer has been evaluated from the variation of the $E^{\circ\prime}$ value with temperature.[23,24] Figure 5 shows the linear correlation found in acetonitrile solution in the temperature range from −20 to +20 °C (correlation coefficients: 0.967 for $[CuL^2]^{2+/+}$; 0.992 for $[CuL^3]^{2+/+}$). An electron-transfer entropy of +32 cal K^{-1} mol^{-1} for $[CuL^2]^{2+/+}$ and of +21 cal K^{-1} mol^{-1} for $[CuL^3]^{2+/+}$ can thus be computed. This positive value confirms that in proposing simple metal complexes as models for the active sites of metallobiomolecules the lack of hydrophilic and/or hydrophobic environments must be taken into account.

The derivatives $[CuL^5{}_2]^{2+}$ to $[CuL^7{}_2]^{2+}$ are unstable in

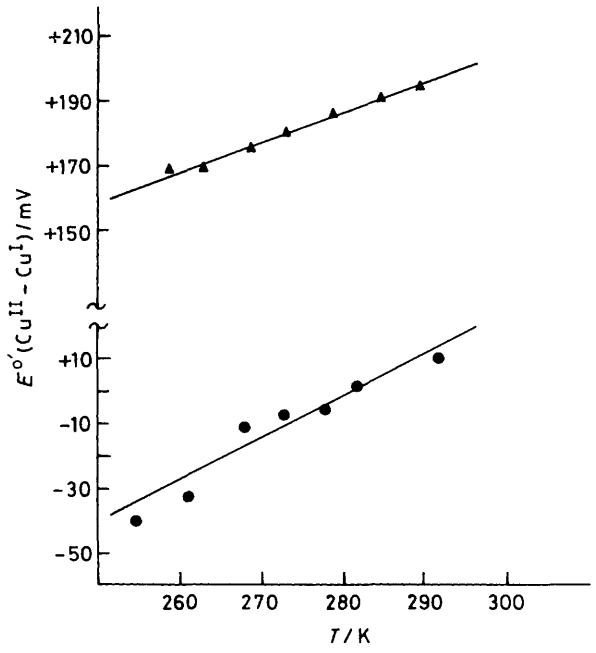

Figure 5. Plots of the Cu^{II}–Cu^{I} redox potential of $[CuL^2]^{2+}$ (●) and $[CuL^3]^{2+}$ (▲) *vs.* temperature in acetonitrile solution

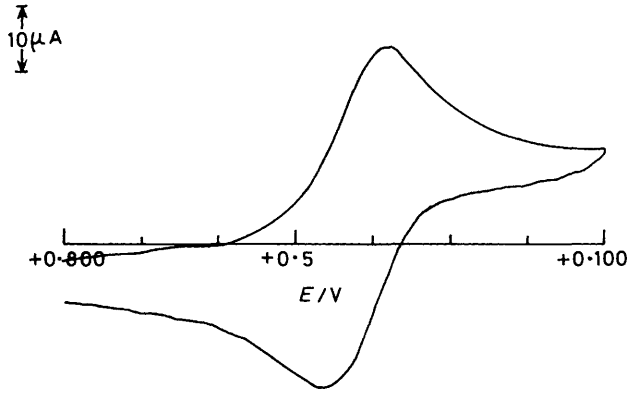

Figure 6. Cyclic voltammogram recorded at a platinum electrode on a deaerated acetonitrile solution containing $[CuL^6{}_2]^{2+}$ (1.00×10^{-3} mol dm^{-3}). Scan rate 0.5 V s^{-1}

dimethylformamide solution; on the contrary, they are sufficiently stable in acetonitrile solution to enable cyclic voltammetric experiments to be performed. As a typical example, Figure 6 shows the cyclic voltammetric response exhibited by $[CuL^6{}_2]^{2+}$. The reduction step Cu^{II}–Cu^{I} obeys the diagnostic criteria for a quasi-reversible electron transfer (i_{p_a}/i_{p_c} constant with scan rate; ΔE_p increases from 90 mV at 0.02 V s^{-1} to 300 mV at 51.2 V s^{-1}; $i_{p_c}v^{-\frac{1}{2}}$ remains practically constant). Also for this complex the two irreversible steps Cu^{I}–Cu^{0} ($E_p = -0.4$ V), and Cu^{II}–Cu^{III} ($E_p = +1.35$ V) are present. As reported in Table 6, this type of complex gives rise to notably high Cu^{II}–Cu^{I} redox potentials, again in accord with the spectroscopic evidence which assigns to the copper(II) complexes (**2**) a structure with significant tetrahedral distortion.[11]

Experimental

Physical Measurements.—Elemental analyses were by the microanalytical laboratory of the University of Milano. Infrared spectra were obtained on a Nicolet MX-1E FT-IR instrument,

Table 6. Redox potentials and peak-to-peak separation for the reduction Cu^{II}–Cu^{I} of the derivatives $[CuL^5{}_2]^{2+}$ to $[CuL^7{}_2]^{2+}$ in acetonitrile solution, at a scan rate of 0.2 V s^{-1}

Complex	$E^{o'}$/V	ΔE_p/mV
$[CuL^5{}_2]^{2+}$	+0.55	270
$[CuL^6{}_2]^{2+}$	+0.43	81
$[CuL^7{}_2]^{2+}$	+0.56	86

Table 7. Crystal and refinement data for $[CuL^2(ClO_4)][ClO_4]$

Formula	$C_{27}H_{24}Cl_2CuN_4O_8S_2$
M	731.15
Space group	$P\bar{1}$
a/Å	16.111(4)
b/Å	11.194(4)
c/Å	8.681(2)
α/°	106.81(2)
β/°	96.47(2)
τ/°	95.38(2)
U/Å^3	1 475.9
Z	2
D_c/g cm^{-3}	1.64
$F(000)$	746
Radiation	Graphite-monochromated Cu-K_α (λ = 1.5418 Å)
Temperature °C	24 ± 3
μ/cm^{-1}	43.2
Scan mode	θ—2θ
Scan speed/° min^{-1}	0.05
Scan width/°	0.9 + 0.3 tan θ
Scan range/°	$1.0 < \theta < 56.0$
Independent reflections	3 398
Observed reflections [$I > 3\sigma(I)$]	3 328
Parameters refined	342
R^a	0.073
R'^b	0.081

^{a} $R = \Sigma(|F_o| - |F_c|)/\Sigma|F_c|$. ^{b} $R' = [\Sigma w(|F_o| - |F_c|)^2/\Sigma w(F_o)^2]^{\frac{1}{2}}$.

with a standard resolution of 2.0 cm^{-1}, electronic spectra on a Perkin-Elmer Lambda-5 spectrophotometer, and proton n.m.r. spectra at 80 MHz on a Bruker WP-80 FT spectrometer. Cyclic voltammetry was performed in a three-electrode cell having a platinum working electrode surrounded by a platinum-spiral counter electrode, and an aqueous saturated calomel reference electrode (s.c.e.) mounted with a Luggin capillary. A BAS 100A electrochemical analyser was used as polarizing unit. Controlled-potential coulometric tests were performed in a H-shaped cell with anodic and cathodic compartments separated by a sintered glass disc. The working macroelectrode was a platinum gauze; a mercury pool was used as counter electrode. An Amel potentiostat model 551, with an associated coulometer (Amel integrator model 558) was employed here. In all electrochemical tests, the temperature was controlled at 20 + 0.1 °C.

Reagents and Preparations.—All reagents were of the highest grade commercially available and were used as received. 3-Formyl-1-phenyl-2(1*H*)-pyridinethione was prepared as described in the literature.[25] Tetrakis(acetonitrile)copper(I) perchlorate was prepared by the usual method.[26] The preparation of the copper(II) complexes was reported previously.[11] The ligand L^1 was obtained by refluxing a mixture of 3-formyl-1-phenyl-2(1*H*)-pyridinethione (1 mmol) and ethylenediamine (0.5 mmol) in absolute ethanol. The product precipitated as a yellow powder.

The complexes of Cu^{I} and Zn^{II} were prepared according to the following general procedure (using an inert atmosphere for Cu^{I}). A solution of the Schiff base was prepared by refluxing a

Table 8. Fractional atomic co-ordinates (× 10^4) for $[CuL^2(ClO_4)][ClO_4]$ with e.s.d.s in parentheses

Atom	*X/a*	*Y/b*	*Z/c*	Atom	*X/a*	*Y/b*	*Z/c*
Cu	3 026(1)	1 694(1)	2 783(1)	C(22)	−116(3)	−3 455(4)	−1 126(6)
S(1)	2 178(1)	1 507(2)	4 668(2)	C(23)	672(3)	−3 578(4)	−386(6)
S(2)	2 009(1)	344(2)	924(2)	C(24)	1 394(3)	−2 867(4)	−564(6)
C(1)	2 447(4)	−271(6)	−793(7)	C(25)	1 327(3)	−2 034(4)	−1 481(6)
N(2)	2 057(3)	−1 390(5)	−1 832(6)	C(26)	535(3)	3 331(4)	6 513(6)
C(3)	2 331(5)	−1 967(7)	−3 287(9)	C(27)	−329(3)	2 928(4)	6 262(6)
C(4)	2 975(5)	−1 405(8)	−3 792(9)	C(28)	−627(3)	1 820(4)	6 567(6)
C(5)	3 383(5)	−278(8)	−2 784(9)	C(29)	−60(3)	1 114(4)	7 123(6)
C(6)	3 157(4)	307(6)	−1 287(7)	C(30)	804(3)	1 517(4)	7 373(6)
C(7)	3 666(4)	1 481(7)	−348(9)	C(31)	1 101(3)	2 625(4)	6 068(6)
N(8)	3 677(3)	2 093(5)	1 152(6)	Cl(1)	2 402(1)	4 965(2)	3 705(6)
C(9)	4 277(5)	3 261(7)	1 800(9)	O(1)	2 357(3)	3 718(5)	2 603(6)
C(10)	5 049(5)	3 065(10)	2 860(10)	O(2)	3 257(4)	5 425(6)	4 411(8)
C(11)	4 834(5)	2 192(8)	3 842(10)	O(3)	1 897(4)	4 951(6)	4 946(8)
N(12)	4 033(3)	2 401(5)	4 469(7)	O(4)	2 083(4)	5 757(5)	2 832(7)
C(13)	4 064(5)	3 061(7)	5 918(9)	Cl(2)	5 909(1)	1 791(2)	−1 615(3)
C(14)	3 370(4)	3 378(6)	6 850(8)	O(5)	5 484(5)	2 893(7)	−1 289(9)
C(15)	3 569(5)	4 342(7)	8 295(9)	O(6)[a]	5 515(9)	815(12)	−985(15)
C(16)	2 988(5)	4 692(8)	9 331(10)	O(7)[b]	6 588(10)	2 246(15)	−172(19)
C(17)	2 207(5)	4 063(7)	8 880(9)	O(8)[c]	6 649(10)	2 095(15)	−2 179(19)
N(18)	1 980(3)	3 123(5)	7 445(6)	O(9)[c]	5 365(11)	1 073(15)	−3 159(19)
C(19)	2 537(4)	2 729(6)	6 359(8)	O(10)[d]	6 202(17)	1 091(25)	−3 023(30)
C(20)	538(3)	−1 910(4)	−2 221(6)	O(11)[e]	6 020(19)	1 287(27)	−354(33)
C(21)	−183(3)	−2 621(4)	−2 044(6)				

Occupancy factors: [a] 0.7; [b] 0.6; [c] 0.5; [d] 0.4; [e] 0.3.

mixture of 3-formyl-1-phenyl-2(1*H*)-pyridinethione (1 mmol) and the appropriate amount of the amine in absolute ethanol (20 cm^3) for about 0.5 h. After cooling to room temperature, the metal perchlorate salt (0.5 mmol) was added as a solid (Cu^I) or dissolved in a small amount of ethanol (Zn^{II}). The resulting mixture was heated for 0.5 h with stirring. Then it was cooled and the brown (Cu^I) or yellow (Zn^{II}) precipitate present was collected by filtration, washed with small amounts of ethanol and diethyl ether, and dried under vacuum. The elemental analyses of the complexes are collected in Table 2.

Crystallographic Study of $[CuL^2(ClO_4)][ClO_4]$.—Crystals of the complex suitable for *X*-ray analysis were obtained by slow diffusion of vapours of diethyl ether into an ethanol solution of the compound at room temperature. A dark brown crystal of approximate dimensions 0.15 × 0.30 × 0.45 mm was chosen for data collection and mounted on an Enraf-Nonius CAD-4 automatic diffractometer. A summary of the crystallographic data is given in Table 7. Unit-cell dimensions were determined from least-squares refinement of the angular settings of 25 carefully centred reflections. Intensities were collected for Lorentz, polarization and absorptions effects[27] (transmission factors ranged between 0.57 and 0.24), and the intensities of three standard reflections were monitored every 120 min for stability control during data collection.

The choice of the $P\bar{1}$ centrosymmetric space group was made on the basis of the centric distribution of *E* values and later confirmed by the refinement of the structure. The structure was solved by the heavy-atom technique, with the use of Patterson and Fourier synthesis. All the hydrogen atoms were located by Fourier difference techniques, but those belonging to the phenyl rings were included in calculated positions in the rigid-group refinement adopted for the rings (see below). Refinement was performed by means of the full-matrix least-squares method. The function minimized was $\Sigma w(|F_o| - |F_c|)^2$ with weights $w = \sigma^{-2}(F_o)$. The two phenyl rings were refined as rigid groups with the hydrogen atoms riding on the corresponding carbons with a common thermal parameter. Anisotropic thermal parameters were refined for all the atoms except the phenyl rings, the oxygen atoms of the perchlorate anions, and the hydrogen atoms. The refinement of the perchlorate counter ion was troublesome because of high rotational disorder around the Cl(2)–O(5) axis. A model with three different orientations of the oxygen atoms in the basal plane of the tetrahedron was constructed; a refinement of this model as three rigid groups was unsuccessful, so the atoms were allowed to move without constraints with fixed approximate occupancies for each oxygen atom. During the last cycle of refinement the maximum shift/error was 0.4 for the *Y/b* parameter of O(11). The final Fourier difference map showed peaks not exceeding 0.8 e $Å^{-3}$ near the disordered perchlorate anion.

All the calculations were performed on an IBM 4361/3 computer with the SHELX 76 set of programs[27] which use the analytical approximation for the atomic scattering factors and anomalous dispersion corrections for all the atoms (from ref. 28). Table 8 gives the final atomic co-ordinates for non-hydrogen atoms with estimated standard deviations (e.s.d.s.) obtained from the least-squares inverse matrix. The molecular plot of Figure 1 was produced by the program ORTEP.[29]

Additional material available from the Cambridge Crystallographic Data Centre comprises H-atom co-ordinates, thermal parameters, and remaining bond lengths and angles.

Acknowledgements

The authors thank the Italian Ministero della Pubblica Istruzione for financial support and P. Illiano for recording n.m.r. spectra.

References

1 (*a*) T. G. Spiro (ed.), 'Copper Proteins,' Wiley, New York, 1981; (*b*) E. T. Adman, *Top. Mol. Struct. Biol.*, 1985, **6**, 1.
2 P. M. Colman, H. C. Freeman, J. M. Guss, M. Murata, V. A. Norris, J. A. M. Ramshaw, and M. P. Venkatappa, *Nature (London)*, 1978, **272**, 319; J. M. Guss and H. C. Freeman, *J. Mol. Biol.*, 1983, **169**, 521.
3 G. E. Norris, B. F. Anderson, and E. N. Baker, *J. Am. Chem. Soc.*, 1986, **108**, 2784.

4 E. T. Adman and L. H. Jensen, *Isr. J. Chem.*, 1981, **21**, 8.
5 H. B. Gray, *Chem. Soc. Rev.*, 1986, **15**, 17; P. Zanello, *Comments Inorg. Chem.*, 1988, **8**, 45.
6 K. D. Karlin and J. Zubieta (eds.), 'Copper Coordination Chemistry: Biochemical and Inorganic Perspectives,' Adenine Press, New York, 1983.
7 J. Reedijk, W. L. Driessen, and J. van Rijn, in 'Biological and Inorganic Copper Chemistry,' eds. K. D. Karlin and J. Zubieta, Adenine Press, New York, 1986, vol. 2, p. 143; J. van Rijn, W. L. Driessen, J. Reedijk, and J-M. Lehn, *Inorg. Chem.*, 1984, **23**, 3584; E. Bouwman, W. L. Driessen, and J. Reedijk, *J. Chem. Soc., Dalton Trans.*, 1988, 1337.
8 (*a*) L. Siegfried and T. A. Kaden, *Helv. Chim. Acta*, 1984, **67**, 29; (*b*) K. P. Balakrishnan, T. A. Kaden, L. Siegfried, and A. D. Zuberbuhler, *ibid.*, p. 1061; (*c*) J. P. Gisselbrecht and M. Gross, *Adv. Chem. Ser.*, 1982, **201**, 109; (*d*) A. W. Addison, T. N. Rao, and E. Sinn, *Inorg. Chem.*, 1984, **23**, 1957; (*e*) M. F. Corrigan, K. S. Murray, B. O. West, and J. R. Pilbrow, *Aust. J. Chem.*, 1977, **30**, 2455; (*f*) A. R. Amundsen, J. Whelan, and B. Bosnich, *J. Am. Chem. Soc.*, 1977, **99**, 6730; (*g*) G. S. Patterson and R. H. Holm, *Bioinorg. Chem.*, 1975, **4**, 257; (*h*) N. Aoi, G. Matsubayashi, and T. Tanaka, *J. Chem. Soc., Dalton Trans.*, 1983, 1059.
9 (*a*) J. Becher, D. J. Brockway, K. S. Murray, P. J. Newman, and H. Toftlund, *Inorg. Chem.*, 1982, **21**, 1791; (*b*) P. Beardwood and J. F. Gibson, *J. Chem. Soc., Chem. Commun.*, 1983, 1099; (*c*) J. Becher, H. Toftlund, and P. H. Olesen, *ibid.*, p. 740; (*d*) O. P. Anderson, J. Becher, H. Frydendahl, L. F. Taylor, and H. Toftlund, *ibid.*, 1986, 699; (*e*) H. Toftlund, J. Becher, P. H. Olesen, and J. Z. Pedersen, *Isr. J. Chem.*, 1985, **25**, 56.
10 R. D. Bereman, M. R. Churchill, and G. Shields, *Inorg. Chem.*, 1979, **18**, 3117; R. D. Bereman, G. D. Shields, J. Bordner, and J. R. Dorfman, *ibid.*, 1981, **20**, 2165; R. D. Bereman, J. R. Dorfman, J. Bordner, D. P. Rillema, P. McCarthy, and G. D. Shields, *J. Inorg. Biochem.*, 1982, **16**, 47.
11 L. Casella, M. Gullotti, and R. Viganò, *Inorg. Chim. Acta*, 1986, **124**, 121.
12 (*a*) L. Casella, *Inorg. Chem.*, 1984, **23**, 2781; (*b*) L. Casella, M. Gullotti, A. Pintar, F. Pinciroli, R. Viganò, and P. Zanello, *J. Chem. Soc., Dalton Trans.*, 1989, 1161.
13 J. S. Thompson, T. J. Marks, and J. A. Ibers, *J. Am. Chem. Soc.*, 1979, **101**, 4180; J. M. Downes, J. Whelan, and B. Bosnich, *Inorg. Chem.*, 1981, **20**, 1081; J. Whelan and B. Bosnich, *ibid.*, 1986, **25**, 3671; P. K. Bharadwaj, J. A. Potenza, and H. J. Schugar, *J. Am. Chem. Soc.*, 1986, **108**, 1351.
14 (*a*) P. K. Bharadwaj, J. A. Potenza, and H. J. Schugar, *J. Am. Chem. Soc.*, 1986, **108**, 1351; (*b*) J. L. Hughey IV, T. G. Fawcett, S. M. Rudich, R. A. Lalancette, J. A. Potenza, and H. J. Schugar, *ibid.*, 1979, **101**, 2617; (*c*) E. John, P. K. Bharadwaj, J. A. Potenza, and H. J. Schugar, *Inorg. Chem.*, 1986, **25**, 3065; (*d*) O. P. Anderson, C. M. Perkins, and K. K. Brito, *ibid.*, 1983, **22**, 1267.
15 K. W. Penfield, R. R. Gay, R. S. Himmelwright, N. C. Eickman, V. A. Norris, H. C. Freeman, and E. I. Solomon, *J. Am. Chem. Soc.*, 1981, **103**, 4382.
16 R. A. Scott, S. P. Cramer, R. W. Show, H. Beinert, and H. B. Gray, *Proc. Natl. Acad. Sci. U.S.A.*, 1981, **78**, 664.
17 E. N. Baker, D. Hall, and T. N. Waters, *J. Chem. Soc. A*, 1970, 406; N. M. Atherton, D. E. Fenton, G. J. Hewson, C. H. McLean, R. Bastida, J. Romero, A. Sousa, and E. E. Castellano, *J. Chem. Soc., Dalton Trans.*, 1988, 1059; N. A. Bailey, R. Bastida, D. E. Fenton, S. J. Lockwood, and C. H. McLean, *ibid.*, p. 839; J. Ellis, G. M. Mockler, and E. Sinn, *Inorg. Chem.*, 1981, **20**, 1206; E. Larsen, S. Larsen, S. Roen, and K. J. Watson, *Acta Chem. Scand. Ser. A*, 1976, **30**, 4; H. M. Dawes, J. M. Waters, and T. N. Waters, *Inorg. Chim. Acta*, 1982, **66**, 29; K. Korhonen and R. Hamalainen, *Acta Crystallogr., Sect. B*, 1981, **37**, 829; R. Hamalainen, U. Turpeinen, M. Ahlgrén, and M. Rantala, *Acta Chem. Scand., Ser. A*, 1978, **32**, 549; R. Hamalainen, M. Ahlgrén, U. Turpeinen, and M. Rantala, *ibid.*, p. 235; K. Korhonen and R. Hamalainen, *ibid.*, 1979, **33**, 569.
18 E. R. Brown and J. Sandifer, in 'Physical Methods of Chemistry, Electrochemical Methods,' eds., B. W. Rossiter and J. F. Hamilton, Wiley, New York, 1986, vol. 2, ch. 4.
19 W. E. Geiger, *Prog. Inorg. Chem.*, 1985, **33**, 275.
20 H. B. Gray and E. I. Solomon, in ref. 1*a*, p. 1.
21 N. Sailasuta, F. C. Anson, and H. B. Gray, *J. Am. Chem. Soc.*, 1979, **101**, 455.
22 J. M. Guss, P. R. Harrowell, M. Murata, V. A. Norris, and H. C. Freeman, *J. Mol. Biol.*, 1986, **192**, 361.
23 E. L. Yee, R. J. Cave, K. J. Guyer, P. D. Tyma, and M. J. Weaver, *J. Am. Chem. Soc.*, 1979, **101**, 1131.
24 M. P. Youngblood and D. W. Margerum, *Inorg. Chem.*, 1980, **19**, 3068.
25 J. Becher and E. G. Frandsen, *Acta Chem. Scand., Ser. B*, 1976, **30**, 863.
26 P. Emmerich and C. Sigwart, *Experientia*, 1963, **19**, 488.
27 G. M. Sheldrick, SHELX 76 Program for Crystal Structure Determination, University of Cambridge, Cambridge, 1976.
28 'International Tables for *X*-Ray Crystallography,' Kynoch Press, Birmingham, 1974, vol. 4.
29 C. K. Johnson, ORTEP, Report ORNL-3794, Oak Ridge National Laboratory, Oak Ridge, Tennessee, 1971.

Received 21*st November* 1988; *Paper* 8/04625E